IChemE
7th WORLD CONGRESS of CHEMICAL ENGINEERING GLASGOW 2005
www.icheme.org/journals
doi: 10.1205/cherd.04346
0263–8762/05/$30.00+0.00

Trans IChemE, Part A, July 2005
Chemical Engineering Research and Design, 83(A7): 915–925

BOUNDING THE STABILITY AND RUPTURE CONDITION OF EMULSION AND FOAM FILMS

J. COONS[1]*, P. HALLEY[2], S. McGLASHAN[2] and T. TRAN-CONG[3]

[1]*Los Alamos National Laboratory, Engineering Sciences and Applications Division, Los Alamos, NM, USA*
[2]*Department of Chemical Engineering, University of Queensland, St Lucia, Australia*
[3]*Faculty of Engineering and Surveying, University of Southern Queensland, Toowoomba, Australia*

A scaling law is presented that provides a complete solution to the equations bounding the stability and rupture of thin films. The scaling law depends on the fundamental physicochemical properties of the film and interface to calculate bounds for the critical thickness and other key film thicknesses, the relevant waveforms associated with instability and rupture, and film lifetimes. Critical thicknesses calculated from the scaling law are shown to bound the values reported in the literature for numerous emulsion and foam films. The majority of critical thickness values are between 15 to 40% lower than the upper bound critical thickness provided by the scaling law.

Keywords: thin films; stability; critical thickness; spontaneous rupture; scaling law.

INTRODUCTION

Despite decades of experimental (Ivanov *et al.*, 1970; Traykov *et al.*, 1977; Rao *et al.*, 1982; Radoev *et al.*, 1983; Manev *et al.*, 1984; Kumar *et al.*, 2002) and theoretical (Vrij, 1966a; Sheludko, 1967; Ivanov *et al.*, 1970; Radoev *et al.*, 1983; Sharma and Ruckenstein, 1987) investigation into the stability and rupture of thin films, very little has been published on their scaling behaviour. Thin liquid films form between the dispersed phase in emulsions and foams and become unstable when long range van der Waals forces induce the growth of capillary waves on the film interfaces (Vrij, 1966a). Upon reaching a critical thickness, films either rupture or shift to a uniform thickness and form a black film (Manev *et al.*, 1974). Vrij (1966a, b) derived limiting equations for the critical thickness under conditions where either the Plateau border pressure drop or disjoining pressure control film drainage. Many films drain under conditions that fit into the intermediate region where both pressure terms are significant and the limiting equations are not applicable. Vrij's unique theoretical approach forced the critical thickness predictions to lower values by applying a wave-averaged corrugation growth rate expression and by specifying the rupture thickness from the film drainage curve at the minimum lifetime. The lower critical thickness predictions were still much larger than the experimental values on aniline and aqueous foam films. In this case, the overprediction was exacerbated by application of Reynolds equation and unusually large Hamacker constants. Vrij used 7×10^{-19} J for aniline and 10^{-19} J for aqueous films, when the non-retarded Hamacker constant predicted from Lifshitz theory is 6.5×10^{-20} J and 3.6×10^{-20} J, respectively (Coons *et al.*, 2005b). Vrij also included an undefined parameter (f), which was inexplicably set to 6.5 and 7 for the validation films. While application of Vrij's limiting equations has the advantage of being relatively simple, frequent discrepancy with experimental results reduce their overall appeal. Ivanov *et al.* (1970) applied the same corrugation growth rate expressions as Vrij, but based the critical condition upon the first waveform to reach the centre of the film. This rupture criterion increases the critical film thickness predictions by 15 to 20% in comparison to Vrij's approach (Coons *et al.*, 2003). A significant limitation of these earlier studies was the absence of a theory that provides accurate film thinning velocities. This limitation persists today, although to a lesser extent (Coons *et al.*, 2005a).

Despite the approximate nature of the equations obtained from linear stability analysis, some studies attempted to validate the theory by achieving close agreement with experimental measurements (Radoev *et al.*, 1983; Sharma and Ruckenstein, 1987). Radoev *et al.* developed a theoretical correlation between the critical film thickness and thinning velocity. Their theoretical approach also yielded a wave-averaged corrugation growth expression and assumed equivalence of the film thinning and corrugation growth velocities at the critical thickness. Sharma and Ruckenstein developed a similar correlation by incorporating the first order corrugation growth rate equation and assuming the equivalence of the film thinning and corrugation growth

*Correspondence to: Dr J. Coons, Los Alamos National Laboratory, Engineering Sciences and Applications Division, P.O. Box 1663, MSC930, Los Alamos, NM 87545, USA.
E-mail: jimc@lanl.gov

velocities. All of these features effect lower critical film thickness predictions. Although the theoretical development in both studies proceeded with reference to the average film thickness, the results were shown to agree closely with the minimum film thickness obtained by accounting for the hydrodynamic corrugations along the film interface. Aside from the juxtaposition of the average and minimum film thicknesses, the main hindrance in applying the resulting correlations is the absence of a general theory for the prediction of the hydrodynamic corrugation amplitude and accurate thinning velocities. Therefore, errors associated with the prediction of thinning velocity bias the prediction of the film thickness. That is, if the thinning velocity is too large, then the correlations will underpredict the critical thickness and vice versa.

In contrast to the above studies, the systems of equations presented in this paper were chosen to bound the stability and rupture conditions. Complete solutions are provided in the form of a scaling law, which is extended beyond the prediction of critical thickness to describe other film thicknesses of interest, the relevant waveforms and drainage times.

BACKGROUND

The time or thickness evolution of a thin film is marked by a series of events as it drains and approaches the critical rupture thickness (Ivanov and Dimitrov, 1988). Each event is associated with either film drainage or the dynamics of interfacial wave growth. Thick films drain in accordance with the Reynolds equation down to what has been referred to in previous work as the Reynolds thickness (Coons *et al.*, 2003). Measurements from a variety of emulsion and foam films confirm that the thinning velocities of most films exceed that predicted by the Reynolds equation (Coons *et al.*, 2005a). This is illustrated in Figure 1 by the ratios of the Reynolds thinning velocity to the measured value, which are less than unity. Likewise, as shown for a variety of foam and emulsion films in Figure 2, the drainage time or the time required to drain between specified thicknesses is generally less than that predicted by the Reynolds equation. A variety of theories have been proposed to account for this discrepancy (Coons *et al.*, 2005a). The drainage theory of Manev *et al.* (1997) or MTsR theory attributes the increased thinning rates to the development of hydrodynamic corrugations along the flexible film interfaces. It is unique amongst other theories in that the existence of corrugations and their correlation with film radius is supported by experimental measurements (Radoev *et al.*, 1983; Manev *et al.*, 1997). MTsR theory predicts that the number of hydrodynamic corrugations in a film, and hence deviation from Reynolds drainage, increases with decreasing film thickness. The Reynolds thickness can be estimated directly from MTsR theory. However, as indicated in Figures 1 and 2, thinning velocities provided by MTsR theory are higher than experimental measurements. Therefore, as was previously observed, the drainage rates of most foam and emulsion films are bounded by the predictions of Reynolds equation and MTsR theory (Coons *et al.*, 2005a).

As a film continues to drain, specific waveforms that comprise interfacial corrugations become unstable and begin to grow in amplitude. The onset of instability occurs at the maximum transition thickness, which is the transition thickness of the waveform that is first to develop a positive growth rate. The instability arises when long range van der Waals (attractive) forces acting between the interfaces overcome the interfacial capillary forces

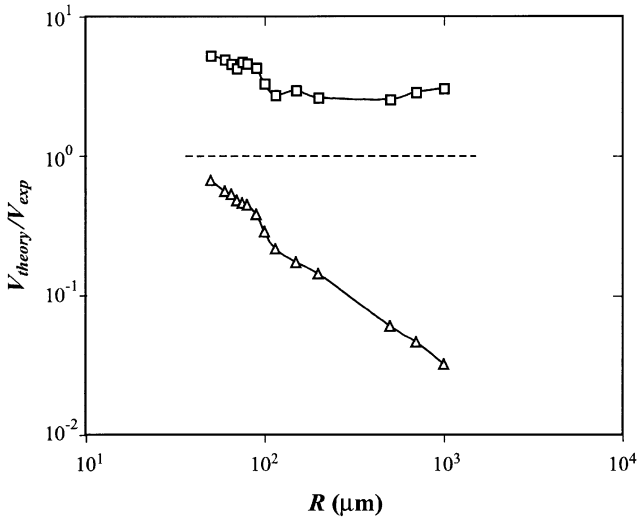

Figure 1. The ratio of the measured film thinning velocity to that predicted by the Reynolds equation (triangles) and MTsR theory (squares) as a function of film radius. The thinning velocities were reported by Radoev *et al.* (1983) for a series of aqueous foam films. The horizontal line indicates agreement between theory and experiment and illustrates that all of the experimental velocity measurements are bounded by those predicted by the Reynolds equation and MTsR theory. All thinning velocities were predicted using the non-retarded Hamaker constant for air–water–air films (3.6×10^{-20} J).

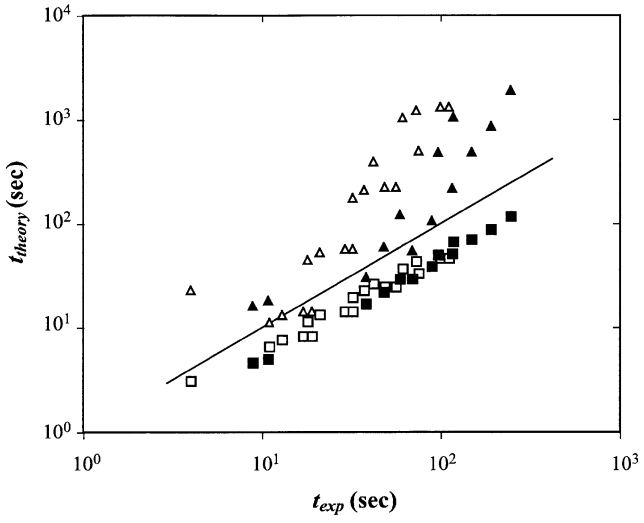

Figure 2. Drainage times reported for a variety of foam films (Manev *et al.*, 1984; Kumar *et al.*, 2002) and emulsion films (Traykov *et al.*, 1977; Manev *et al.*, 1984) as compared to the drainage times predicted from the Reynolds equation (triangles) and MTsR theory (squares). Drainage times of foam films are indicated by open symbols and those of emulsion films by closed symbols. The solid line indicates agreement between theory and experiment and further illustrates that most experimental measurements are bounded by the drainage theories. Drainage times reported by Manev *et al.* (1984) for films of radius 50 μm are slightly lower than predictions from the Reynolds equation, and are located slightly below the line of agreement. All drainage times were predicted using the non-retarded Hamaker constant and parameters reported by Coons *et al.* (2005b) for each film system.

acting to smooth out the corrugations. As the film continues to drain, additional waveforms become unstable. Each unstable waveform grows at a unique rate, and if given the chance, would cause the film to rupture at different times and (average) thicknesses. By definition, the critical waveform is the first waveform to reach the middle of the film and hence provides the maximum critical rupture thickness of all waveforms.

In the absence of robust computational codes and precise boundary conditions, approximate expressions were introduced in the earliest studies of spontaneous rupture to describe the destabilization and rupture dynamics. These early theoretical investigations effectively replaced the nonlinear terms of the local film thickness (H) in the evolution equation by approximate expressions with a linear dependency on wave amplitude ($\zeta_0\zeta$). For example, a first order approximation is given by the following expression where h is the average film thickness.

$$H^3 = h^3\left[1 - \left(\frac{2\zeta_0\zeta}{h}\right)\right]^3 \approx h^3\left[1 - 3\left(\frac{2\zeta_0\zeta}{h}\right)\right] \qquad (1)$$

Substitution of the first order approximate leads to a velocity dependent wave growth rate expression consistent with linear stability theory (Gumerman and Homsy, 1975; Sharma and Ruckenstein, 1987; Coons *et al.*, 2003). In a previous review, it was shown that the corrugation growth rate expression obtained by neglecting the effect of thinning velocity is the same expression derived by introducing a zeroth order (h^3) function (Coons *et al.*, 2003). The zeroth order or non-thinning wave growth rate expression appears in several earlier studies on thin film rupture (Vrij, 1966a; Ivanov *et al.*, 1970; Radoev *et al.*, 1983). Comparison of the zeroth and first order approximations to the fully expanded nonlinear function in equation (1) shows that the approximate functions bound the actual value as the amplitude of the wave approaches the film thickness. It is assumed in the subsequent theoretical section that conditions describing the capillary wave growth are bounded by the expressions obtained from the introduction of these approximate functions. It was recently shown (Coons *et al.*, 2005b) and is again indicated in Figure 3, that the critical thicknesses of a variety of emulsion and foam films are bounded by selectively coupling existing drainage theory with the approximate corrugation growth rate expressions. Before presenting the scaling law, we first describe the underlying equations that bound the drainage and rupture conditions.

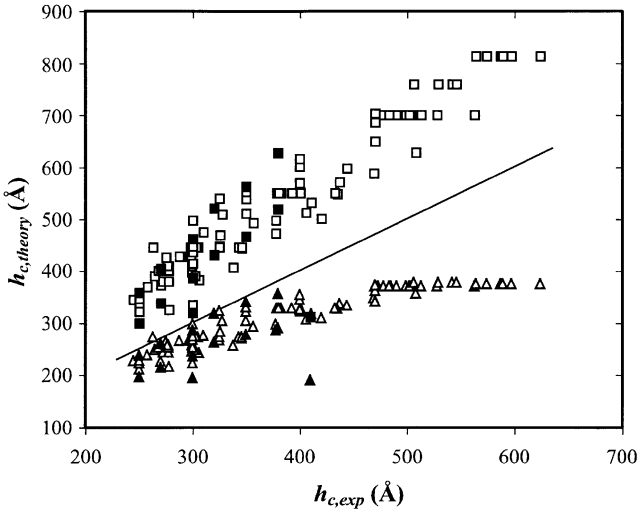

Figure 3. Critical thickness measurements reported for numerous foam (Exerowa and Kolarov, 1966; Vrij, 1966a; Scheludko and Manev, 1968; Rao *et al.*, 1982; Radoev *et al.*, 1983; Manev *et al.*, 1984; Kumar *et al.*, 2002) and emulsion (Traykov *et al.*, 1977; Manev *et al.*, 1984) films compared to scaling law predictions for the upper (square) and lower (triangle) critical film thickness. Thickness measurements on foam films are indicated by open symbols and those on emulsion films by closed symbols. The solid line indicates agreement between theory and experiment and illustrates that most measurements are bounded by the upper and lower critical film thicknesses predicted by the scaling law with constants provided in Table 1. Traykov *et al.* (1977) reported a critical thickness of 410 Å for emulsion film number 1, which is much larger than the predicted upper bound.

THE BOUNDING EQUATIONS

The theoretical origin of the equations used in this work to approximate film thinning and corrugation growth dynamics has been described previously (Coons *et al.*, 2003). Here, only the system of equations used to bound the stability and critical rupture condition are presented.

Bounding the conditions that mark the onset of instability and rupture in free-standing thin films requires consideration of two underlying dynamics; (1) drainage of the liquid from the perimeter of the film and the resultant film thinning, and (2) growth of capillary waves on the film interfaces. If a film is draining at a slow rate and the capillary waves are growing at a fast rate, then the critical or rupture thickness will be thicker than if the relative rates of the two underlying dynamics were reversed. Therefore, combination of the equations that provide the slowest film drainage and the fastest corrugation growth leads to the upper bound of the maximum transition and critical thicknesses. The upper bound of the critical film thickness is given by the following equation, where time or $\int \mathrm{d}t$ is replaced with $-\int \mathrm{d}h/V$.

$$h_{\mathrm{c,upper}} = 2\zeta_0 \exp\left(\frac{\alpha_{\mathrm{crit}}^2}{24\mu R^2}\int_{h_{\mathrm{c,upper}}}^{h_t}\left[\frac{A}{\pi h} - \frac{\sigma\alpha_{\mathrm{crit}}^2 h^3}{R^2}\right]\frac{\mathrm{d}h}{V_{\mathrm{Re}}}\right) \qquad (2)$$

A is the non-retarded Hamaker constant, $h_{\mathrm{c,upper}}$ is the upper bound of the critical film thickness or the average film thickness at the rupture condition, R is the film radius, and μ is the bulk viscosity of the film fluid. The thickness dependence of the Hamaker constant typically becomes more significant when the film thickness decreases below 1000 Å. However, it was previously determined that application of the non-retarded Hamaker constant more effectively bounded thin films over the range of sizes that have been reported in the literature (Coons *et al.*, 2005b). ζ_0 is the initial amplitude of the capillary wave and is estimated assuming that the corrugation results from the thermal motion of the molecules along the interface (Radoev *et al.*, 1983).

$$\zeta_0 = \sqrt{k_{\mathrm{B}}T/\sigma} \qquad (3)$$

k_B is the Boltzmann constant, T is absolute temperature, and σ is the interfacial tension. h_t in equation (2) is the transition thickness of the critical wave and is related to the dimensionless root of the critical wave (α_{crit}) by the following equation.

$$\alpha_{crit} = R\left(\frac{A}{\pi\sigma h_t^4}\right)^{1/2} \tag{4}$$

Equation (4) represents the relationship between the root of any wave and its corresponding transition thickness, when equation (2) is in use. The root of the critical wave is identified by optimizing equation (2) with respect to α_{crit}, which results in the following equation.

$$\alpha_{crit}^2 \int_{h_{c,upper}}^{h_t} \frac{h^3 dh}{V_{Re}} = \frac{AR^2}{2\pi\sigma} \int_{h_{c,upper}}^{h_t} \frac{dh}{hV_{Re}} \tag{5}$$

V_{Re} is the film thinning velocity as provided by the Reynolds equation, which typically underpredicts the thinning velocities of foam and emulsion films.

$$V_{Re} = -\frac{dh}{dt} = \frac{2h^3\Delta P}{3\mu R^2} \tag{6}$$

h is the average film thickness and ΔP is the drainage pressure or the average radial pressure drop across the film. In the absence of electrostatic repulsion, the drainage pressure has two components; the Plateau border pressure drop and the intrafilm disjoining pressure. The Plateau border pressure drop is the pressure drop at the perimeter of the film due to the curvature of the meniscus. Attractive van der Waals forces act on the film interfaces to create a negative disjoining pressure within the film. The drainage pressure is given by the following expression.

$$\Delta P = 2\sigma\left(\frac{R_c}{R_c^2 - R^2}\right) + \frac{A}{6\pi h^3} \tag{7}$$

R_c is the radius of the capillary tube. The first term on the right hand side of equation (7) is the Plateau border pressure drop and the second term is the disjoining pressure. In a film of constant radius, the Plateau border pressure drop is not time dependent, whereas the disjoining pressure component increases as the film thickness decreases. The dominant component of the drainage pressure is determined by the physicochemical properties as well as the range of thickness that the film experiences over its lifetime. Coons *et al.* (2003) have shown that for films of large radii, the Plateau border pressure drop term dominates throughout the unstable period up to the point of rupture. For small radii films, the disjoining pressure contributes more significantly but never completely dominates the drainage pressure. Equations (2) through (7) constitute the system of equations required to determine the upper bound of the critical film thickness, which is identical to the theory described by Ivanov *et al.* (1970) when the disjoining pressure has a $1/h^3$ dependency.

Solution of the above system of equations also provides the transition thickness of the critical wave. However, the critical wave is generally not the first wave to become unstable and hence, its transition thickness does not represent the initial onset of instability in the film. The first wave to become unstable is identified by optimizing the transition thickness in equation (4) with respect to α, which leads to the Frenkel criterion for film stability.

$$h_{t,0}^{max} = \left[\frac{A}{\pi\sigma}\left(\frac{R}{\alpha_1}\right)^2\right]^{1/4} \tag{8}$$

α_1 is the first root of the Bessel function of first kind order zero, and is approximately 2.4048. The zero in the subscript of the maximum transition thickness denotes the upper bound that is derived from the zeroth order corrugation growth rate, which neglects the effect of thinning velocity on film stability. Films become unstable when they thin below the maximum transition thickness. Therefore, equation (8) provides the upper bound of film thickness at which the film becomes unstable.

A film's lifetime or the time that it spends in an unstable state can be estimated by integrating the derivative of time from the onset of the first instability to the time of rupture. Replacement of $\int dt$ with $-\int dh/V$ in equation (6) provides the following expression for the upper bound of a film's lifetime.

$$t_{l,upper} = -\int_{h_{t,0}^{max}}^{h_{c,upper}} \frac{dh}{V_{Re}} \tag{9}$$

The lower bound of the critical thickness is determined by combining the equations that provide the slowest corrugation growth and the fastest film drainage. Therefore, the first order corrugation growth rate expression (Sharma and Ruckenstein, 1987) is coupled with MTsR theory to provide the lower bound of the critical film thickness.

$$h_{c,lower} = 2\zeta_0 \exp\left(\frac{\alpha_{crit}^2}{24\mu R^2}\int_{h_{c,lower}}^{h_t}\left[\frac{A}{\pi h} - \frac{\sigma\alpha_{crit}^2 h^3}{R^2}\right] \times \frac{dh}{V_{MTsR}} - 3\int_{h_{c,lower}}^{h_t}\frac{dh}{h}\right) \tag{10}$$

The first order corrugation growth rate expression provides a different relationship between the root of a wave and its transition thickness. For the critical wave, this becomes:

$$\alpha_{crit}^4 - \left(\frac{AR^2}{\pi\sigma h_t^4}\right)\alpha_{crit}^2 + \frac{72\mu R^4 V_{MTsR}}{\sigma h_t^4} = 0 \tag{11}$$

The root of the critical wave is identified as before, that is, by optimizing the critical thickness in equation (10) with respect to α. As is apparent by comparison of equations (2) and (10), the root of the critical wave for the lower bound is also given by equation (5), with the appropriate thinning velocity expression inserted.

$$\alpha_{crit}^2 \int_{h_{c,lower}}^{h_t} \frac{h^3 dh}{V_{MTsR}} = \frac{AR^2}{2\pi\sigma} \int_{h_{c,lower}}^{h_t} \frac{dh}{hV_{MTsR}} \tag{12}$$

V_{MTsR} is the film thinning velocity provided by the theory of Manev *et al.* (1997).

$$V_{MTsR} = V_{Re} l^{3/2} \tag{13}$$

l is the theoretical number of domains or rings that form as the film thins and is given by the following theoretical expression.

$$l = \left[\frac{\Delta P}{h\sigma}\left(\frac{R}{4}\right)^2\right]^{2/5} \geq 1 \tag{14}$$

Equations (13) and (14) form the theoretical MTsR equation. Equations (3), (6), (7), and (10) through (14) constitute the system of equations required to determine the lower bound of the critical film thickness.

The lower bound of the maximum transition thickness ($h_{t,1}^{max}$) is obtained by optimizing the transition thickness in equation (11) with respect to the wave root.

$$h_{t,1}^{max} = \left[\frac{A\alpha_1^2/6\pi(h_{t,1}^{max})^3}{32(l|_{h_{t,1}^{max}})^{3/2}\Delta P|_{h_{t,1}^{max}}}\right]^{1/4} h_{t,0}^{max} \tag{15}$$

The subscript t,1 denotes the lower bound obtained from the first order corrugation growth rate.

The lower bound of a film's lifetime was estimated from the following expression.

$$t_{l,lower} = -\int_{h_{t,1}^{max}}^{h_{c,lower}} \frac{dh}{V_{MTsR}} \tag{16}$$

THE THIN FILM SCALING LAW

Solution of the systems of equations was obtained after converting the equations into dimensionless form using the following parameters.

$$h_{t,0}^* = \frac{h_{t,0}^{max}}{2\zeta_0} \tag{17}$$

$$h_{t,1}^* = \frac{h_{t,1}^{max}}{2\zeta_0} \tag{18}$$

$$h_{c,upper}^* = \frac{h_{c,upper}}{2\zeta_0} \tag{19}$$

$$h_{c,lower}^* = \frac{h_{c,lower}}{2\zeta_0} \tag{20}$$

$$h_t^* = \frac{h_t}{2\zeta_0} \tag{21}$$

$$P^* = \frac{A(R_c^2 - R^2)}{12\pi\sigma(2\zeta_0)^3 R_c} \tag{22}$$

$$\tau_{l,upper}^* = \frac{A^2 t_{l,upper}}{24\pi^2\mu\sigma(2\zeta_0)^5} \tag{23}$$

$$\tau_{l,lower}^* = \frac{A^2 t_{l,lower}}{24\pi^2\mu\sigma(2\zeta_0)^5} \tag{24}$$

The superscript asterisk indicates that the parameter is dimensionless. The resulting equations were then solved over a broad input parameter space [P^*, $h_{t,0}^*$:$10^2 - 10^{11}$, $25 - 2500$] employing the following algorithm. For a given [P^*,$h_{t,0}^*$] pair, $h_{t,1}^*$ was determined by minimizing the sum of the square of error from the dimensionless form of equation (15) using the Solver tool in Microsoft® Office Excel 2003. The upper bound of the critical thickness was determined for a given [P^*, $h_{t,0}^*$] pair by first guessing the critical and transition thickness. α_{crit} was then calculated from equation (4) and a forward difference scheme was employed with equation (5) to determine a new transition thickness. The process was repeated until the relative difference between the new and previous transition thicknesses was less than 10^{-8}. Equation (2) was then used with a forward difference scheme to calculate a new $h_{c,upper}^*$ and the procedure to determine h_t^* was repeated. Solution was assumed when the relative error between the new and previous critical thickness values was less than 10^{-8}. Calculation of $h_{c,lower}^*$ followed the same algorithm using equations (10)–(12). The integrals in equations (2), (5), (9), (10), (12), and (16) were evaluated using the IMSL DQDAGS subroutine from Visual Numerics (copyright dated 1997).

The following scaling law emerges from the self-similarity of the calculated dimensionless transition and critical film thicknesses, wave root, and drainage times.

$$S^* = C(h_{t,0}^*)^x (P^*)^y \tag{25}$$

S^* is one of the dimensionless variables in the solution set listed in Table 1. The constants C, x, and y are dependent on the system of equations solved and the master curve approximation within a given drainage subdomain. The shifted data and approximate master curves for all relevant dimensionless parameters are shown in Figure 4, and the shift factors are provided in Table 2. Calculation of the input parameters $h_{t,0}^*$ and P^* require five physicochemical properties; the non-retarded Hamaker constant (A), the radius of the film (R), the radius of the capillary tube (R_c) or the radius of curvature of the Plateau border interface, the absolute temperature (T), and the interfacial tension (σ). As was pointed out by Vrij (1966a), film thickness predictions using the above equations do not require the film viscosity as long as the film thinning rate is inversely proportional to μ. However, conversion of the dimensionless lifetime into dimensional time does require the viscosity of the film medium.

DISCUSSION

The computational ease of the scaling law comes with the cost of increased error. This is apparent in Figure 4 where discrepancies between the computed values and the approximated master curves exist near the subdomain boundaries and in the region where both the Plateau border pressure drop and the disjoining pressure components contribute to the drainage pressure. The magnitude of the error can be determined by comparing the results obtained from the computational algorithm ($S_{computed}^*$) to those obtained from the scaling law ($\widehat{S^*}$) over the input parameter space investigated. The relative error (e)

Table 1. Scaling law constants for the prediction of the dimensionless parameter S^*.

S^*	Description	z	Subdomain boundary	Dominant film pressure term[1]	C	x	y
h^*_{Re}	The upper bound of the Reynolds film thickness	$\frac{P^*}{(h^*_{t,0})^3}$	$z \geq 0.485$	D	0.515	1	0
			$0.485 > z > 0.0759$	D and P	0.407	1.979	−0.326
			$z \leq 0.0759$	P	0.0716	4	−1
$h^*_{t,0}$	The upper bound film thickness marking the onset of instability	—	—	—	1	1	0
$h^*_{t,upper}$	The upper bound transition thickness of the critical wave	$\frac{P^*}{(h^*_{t,0})^{2.859}}$	$z \geq 2.061$	D	0.767	0.944	0
			$2.061 > z > 0.0361$	D and P	0.728	0.735	0.0731
			$z \leq 0.0361$	P	0.912	0.548	0.138
$h^*_{c,upper}$	The upper bound critical film thickness	$\frac{P^*}{(h^*_{t,0})^{2.861}}$	$z \geq 1.239$	D	0.514	0.944	0
			$1.239 > z > 0.0190$	D and P	0.506	0.735	0.0731
			$z \leq 0.0190$	P	0.656	0.548	0.138
$\tau^*_{l,upper}$	The upper bound film lifetime	$\frac{P^*}{(h^*_{t,0})^{2.9}}$	$z \geq 4.169$	D	3.459	5.019	0
			$4.169 > z > 0.077$	D and P	2.102	4.011	0.348
			$z \leq 0.077$	P	5.336	2.957	0.711
$h^*_{t,1}$	The lower bound film thickness marking the onset of instability	$\frac{P^*}{(h^*_{t,0})^{3.069}}$	$z \geq 1.318$	D	0.656	0.998	0
			$1.318 > z > 0.0114$	D and P	0.633	0.590	0.133
			$z \leq 0.0114$	P	1.026	0.258	0.241
$\alpha_{t,1}$	Root of the waveform that provides the lower bound of the onset of instability	$\frac{P^*}{(h^*_{t,0})^{2.989}}$	$z \geq 1.296$	D	4	0	0
			$1.296 > z > 0.0643$	D and P	3.726	−0.710	0.237
			$z \leq 0.0643$	P	7.478	−1.458	0.488
$h^*_{t,lower}$	The lower bound transition thickness of the critical wave	$\frac{P^*}{(h^*_{t,0})^{2.786}}$	$z \geq 2.785$	D	0.773	0.912	0
			$2.785 > z > 0.024$	D and P	0.675	0.541	0.133
			$z \leq 0.024$	P	1.009	0.240	0.241
$h^*_{c,lower}$	The lower bound critical film thickness	$\frac{P^*}{(h^*_{t,0})^{2.735}}$	$z \geq 1.994$	D	0.491	0.899	0
			$1.994 > z > 0.0172$	D and P	0.448	0.535	0.133
			$z \leq 0.0172$	P	0.695	0.240	0.241
$\tau^*_{l,lower}$	The lower bound film lifetime	$\frac{P^*}{(h^*_{t,0})^{2.925}}$	$z \geq 1.639$	D	1.503	5.021	0
			$1.639 > z > 0.0796$	D and P	1.091	3.122	0.649
			$z \leq 0.0796$	P	4.298	1.531	1.193

[1]Disjoining pressure (D) or Plateau border pressure drop (P).

provided by the scaling law is defined below.

$$e = \left[\frac{\widehat{S^*} - S^*_{computed}}{\widehat{S^*}}\right] \times 100\% \tag{26}$$

The relative error determined for all computed values is shown in Figure 5(a)–(e). As expected, the error introduced by the scaling law is very dependent on the position along the master curve, which is stipulated by the input parameters in the form of the dimensionless parameter z. For example, at high z values along the flat portion of the master curve, most of the scaling laws provide values that are within 2% of the computed value. At low to moderate z values, scaling law predictions differ by as much as 15% for film thicknesses or 28% for film lifetimes, compared to the computed values. The scaling law provides the least error for the upper bound values in Figure 5(a), which are within $\pm 3.5\%$ of the computed value. The error provided by the scaling law is not unreasonable given that the purpose of this analysis is to bound the stability and rupture conditions.

The thin film scaling law is a simple tool that provides approximate bounds for the events that mark the time evolution of a draining film. To demonstrate its application, film thickness and lifetime predictions for the foam films of Radoev *et al.* (1983) are shown in Figures 6 and 7, respectively. The curve in Figure 6(a) represents the Reynolds thickness predicted by MTsR theory. The scaling law constants for the Reynolds thickness were reported previously under limiting conditions (Coons *et al.*, 2003), and are provided in Table 1 for the entire range of drainage conditions. The Reynolds film thickness for each film is well above the average critical film thickness indicated by the data points. It should be noted that the thickness at which a given film forms in a capillary cell apparatus is not generally reported. Therefore, the Reynolds thickness and other reference thicknesses discussed here may not have actually existed in the film's history. Without equations describing the film hydrodynamics and boundary conditions, the exact film thickness marking the onset of instability can not be calculated. Here, we speculate that the onset of instability is bounded by the upper and lower maximum transition thickness shown in Figure 6(b). The lower bound maximum transition thickness is consistently higher than the transition and critical thickness of the lower bound critical wave shown in Figure 6(d). The upper bound of the maximum transition thickness for all of the films exceeds 1000 Å, which is occasionally mentioned as the approximate thickness that long range van der Waals forces become significant (Israelachvili, 1992). The transition and critical thicknesses of the upper bound critical wave in Figure 6(c) display a parallel film radius

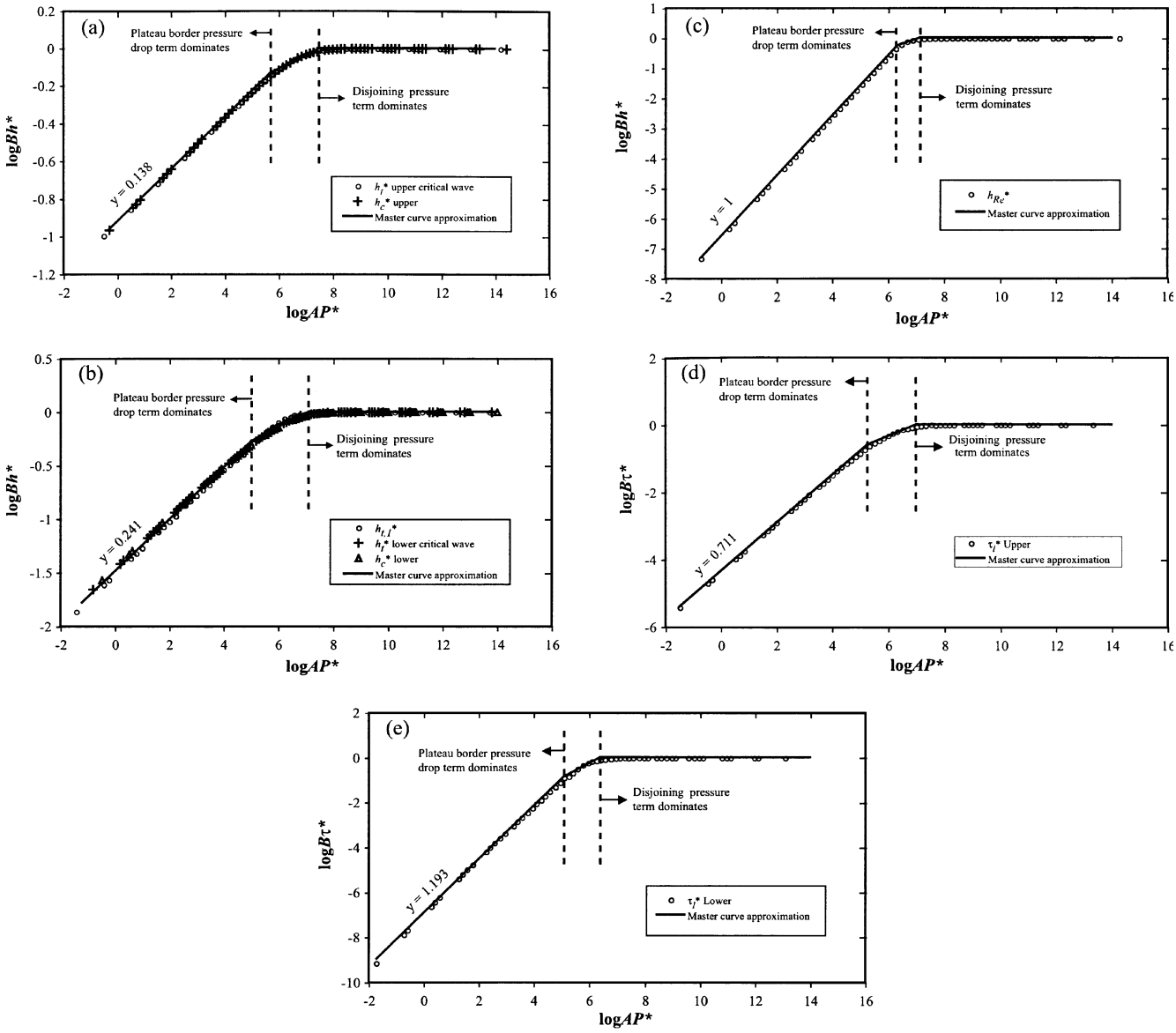

Figure 4. The master curves formed by shifting the computed values both vertically and horizontally using the shift factors, A (horizontal) and B (vertical), in Table 2. The solid lines represent the approximate master curves over each subdomain. Master curves are shown for (a) the transition and critical thickness of the upper critical wave, (b) the maximum transition thickness and the transition and critical thickness of the lower critical wave, (c) the Reynolds thickness, (d) the upper film lifetime, and (e) the lower film lifetime.

dependency as do the lower bound thicknesses in Figure 6(d). This is also apparent by inspecting the scaling law constants in Table 1, where only the pre-exponential constant of the transition and critical thickness varies significantly in a given subdomain. The scaling law predictions of the critical film thickness consistently bound the average critical rupture thicknesses shown in Figure 6(c) and (d).

The film lifetimes of Figure 7 provide an indication of the thinning dynamics for the foam films of Radoev *et al.*

Table 2. Shift factors for the dimensionless parameter S^*.

S^*	Description	log A	log B
h^*_{Re}	The upper bound of the Reynolds film thickness	$-3\log h^*_{\mathrm{t,0}} + 7.468$	$-\log h^*_{\mathrm{t,0}} + 0.288$
$h^*_{\mathrm{t,upper}}$	The upper bound transition thickness of the critical wave	$-2.859\log h^*_{\mathrm{t,0}} + 7.212$	$-0.944\log h^*_{\mathrm{t,0}} + 0.115$
$h^*_{\mathrm{c,upper}}$	The upper bound critical film thickness	$-2.861\log h^*_{\mathrm{t,0}} + 7.433$	$-0.944\log h^*_{\mathrm{t,0}} + 0.289$
$\tau^*_{\mathrm{l,upper}}$	The upper bound film lifetime	$-2.900\log h^*_{\mathrm{t,0}} + 6.380$	$-5.019\log h^*_{\mathrm{t,0}} - 0.539$
$h^*_{\mathrm{t,l}}$	The lower bound film thickness marking the onset of instability	$-3.069\log h^*_{\mathrm{t,0}} + 6.994$	$-0.998\log h^*_{\mathrm{t,0}} + 0.183$
$h^*_{\mathrm{t,lower}}$	The lower bound transition thickness of the critical wave	$-2.795\log h^*_{\mathrm{t,0}} + 6.683$	$-0.912\log h^*_{\mathrm{t,0}} + 0.112$
$h^*_{\mathrm{c,lower}}$	The lower bound critical film thickness	$-2.738\log h^*_{\mathrm{t,0}} + 6.842$	$-0.899\log h^*_{\mathrm{t,0}} + 0.309$
$\tau^*_{\mathrm{l,lower}}$	The lower bound film lifetime	$-2.925\log h^*_{\mathrm{t,0}} + 6.199$	$-5.021\log h^*_{\mathrm{t,0}} - 0.177$

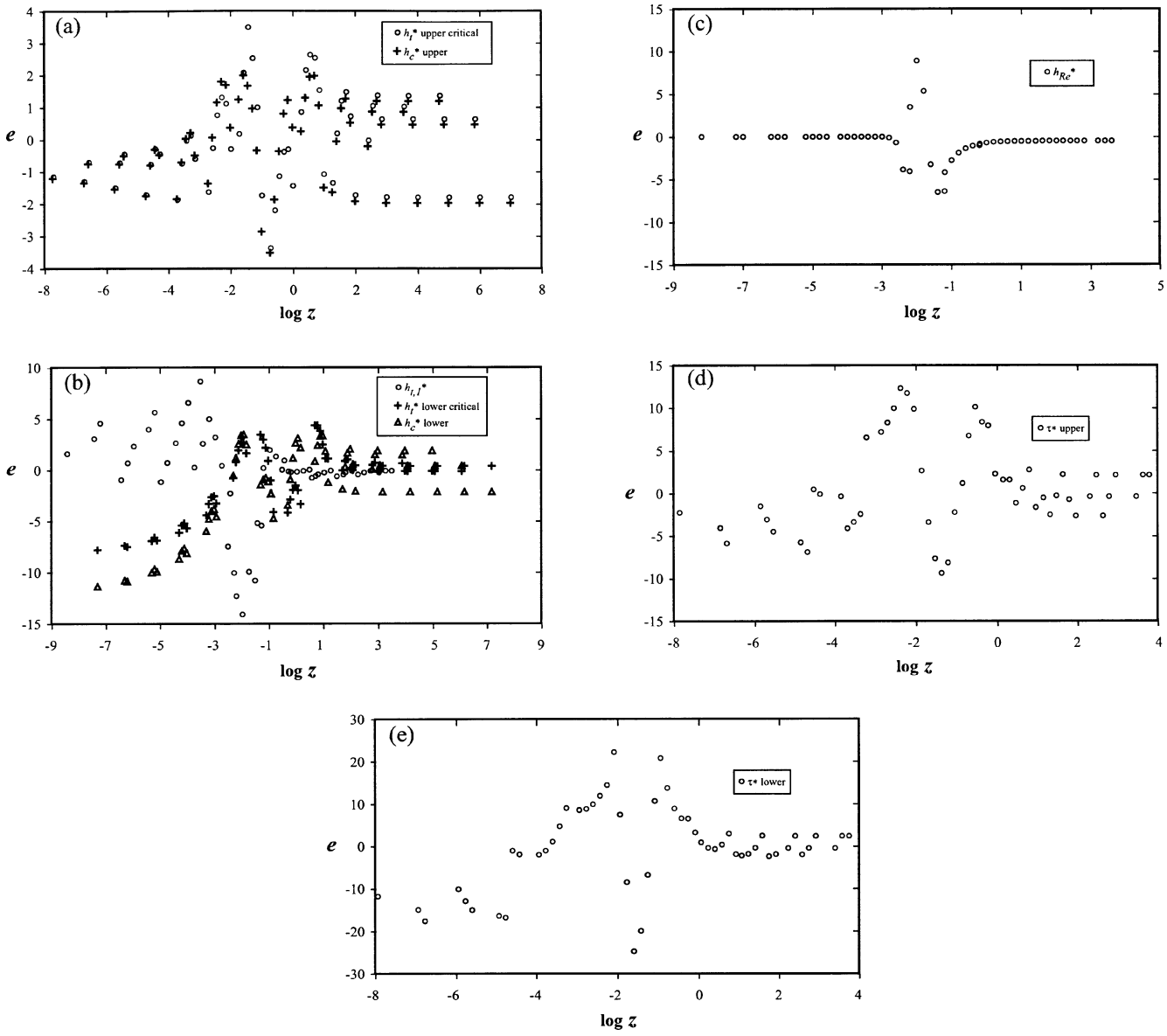

Figure 5. The relative errors obtained by use of the scaling laws as compared to the values computed from the set of equations. With the exception of the lower bound critical thickness, the largest error is typically observed within the subdomain in which both disjoining pressure and the Plateau border pressure drop terms dominate the film drainage pressure. The sequence (a) through (e) is the same as in Figure 4.

(1983). Assuming that the thickness history of the film includes the upper bound of the maximum transition thickness, the time period of instability for the smallest film is estimated to be between 13 and 77 seconds, and between 1.3 and 77 minutes for the largest film. The lower bound lifetime may serve as a criterion for the relevance of spontaneous rupture in surfactant stabilized liquid foams or froths that do not permit accurate measurements of film thickness. That is, if the film lifetime is larger than the minimum lifetime estimated by the scaling equation, then spontaneous rupture should be considered amongst other potential mechanisms for rupture.

Waveforms responsible for the instability and rupture can also be approximated by the scaling law. Waveforms with the longest wavelengths are provided from the zeroth order growth rate expression. The root of the wave that first becomes unstable for the upper bounding equation set is always α_1, whereas the root of the critical wave is given by substituting the transition thickness of the upper bound critical wave into equation (4). Waveforms with the smallest wavelengths are provided from the first order growth rate expression. The root of the wave that first becomes unstable as determined by the lower bounding equation set is provided as a scaling law in Table 1. The root of the critical wave for the lower bounding equation set is determined from the following equation.

$$\alpha_{\text{crit}} = \left[\frac{\alpha_1^2}{2}\left(\frac{h_{\text{t},0}^*}{h_{\text{t}}^*}\right)^4 + \left\{\frac{\alpha_1^4}{4}\left(\frac{h_{\text{t},0}^*}{h_{\text{t}}^*}\right)^8 - \left(3\alpha_1^2\left(\frac{h_{\text{t},0}^*}{h_{\text{t}}^*}\right)^4\left[\frac{P^* + (h_{\text{t}}^*)^3}{P^*}\right]\right)^{8/5}\right\}^{1/2}\right]^{1/2} \quad (27)$$

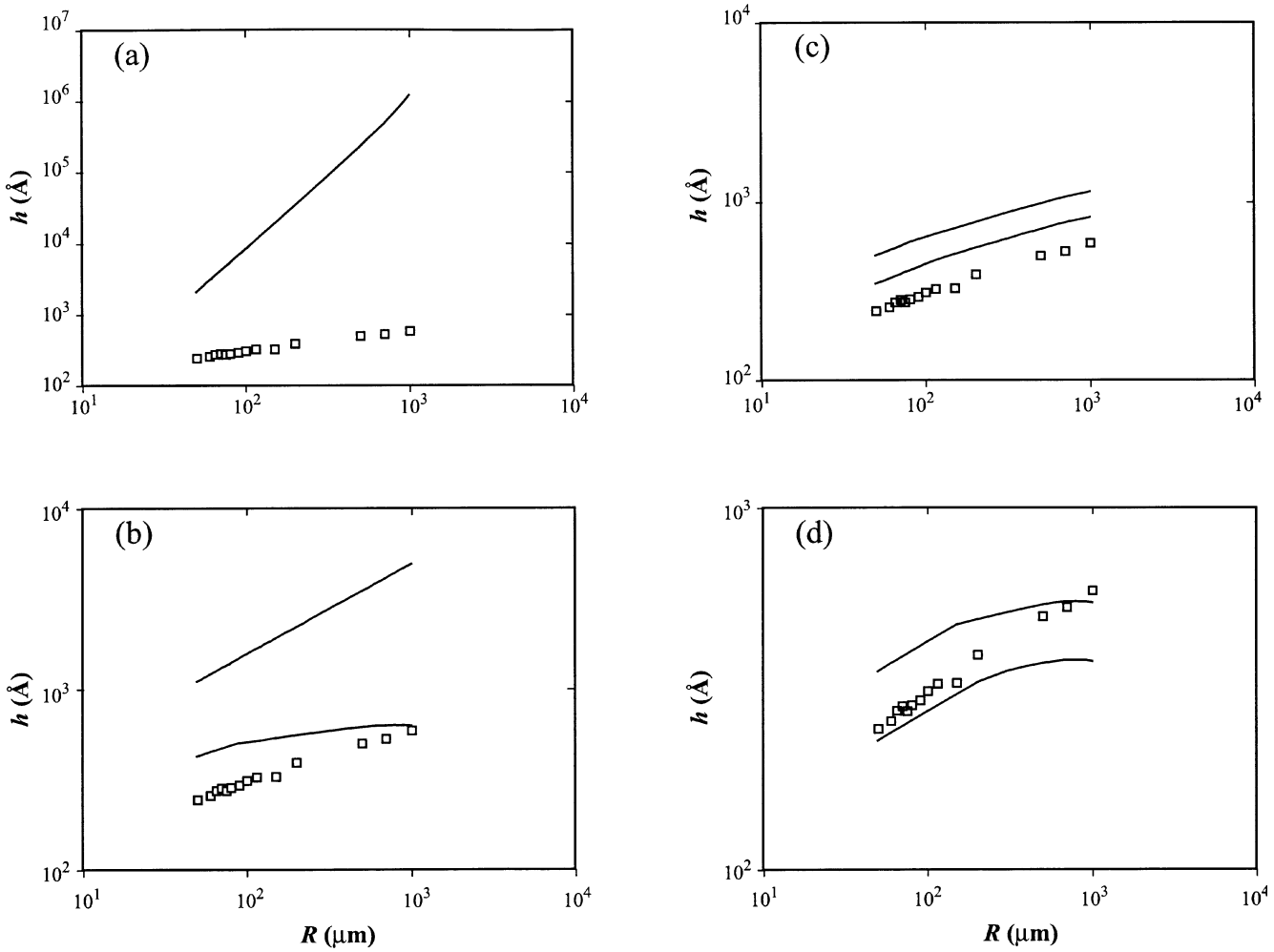

Figure 6. A comparison of the critical film thicknesses reported by Radoev *et al.* (1983) to various film thicknesses obtained from the scaling law. The average critical thickness values reported for the series of foam films are shown as square symbols. The sequence (a)–(e) illustrates the drainage and stability events of each film as it thins to the point of rupture. The solid curves indicate (a) the Reynolds thickness, (b) the upper and lower bound of the maximum transition thickness, (c) the transition (upper curve) and critical thickness (lower curve) of the upper bound critical wave, and (d) the transition (upper curve) and critical thickness (lower curve) of the lower bound critical wave.

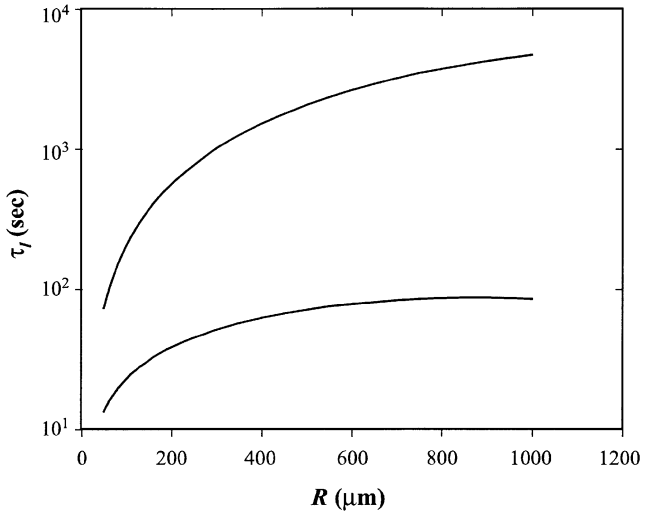

Figure 7. The upper and lower lifetime estimates for the foam films of Radoev *et al.* (1983). The lifetime is the time period over which the film is unstable.

Once the root (α_n) is known, the shape of the waveform along the interface can be plotted as a function of radial position r.

$$\zeta(r) = -J_0\left(\frac{\alpha_n r}{R}\right) \tag{28}$$

J_0 is the Bessel function of first kind order zero. The root of the wave is related to its wavenumber (n) by the following equation.

$$\alpha_n \approx \pi(n - 1/4) \tag{29}$$

As is indicated in Figures 3 and 6(c), the upper bound estimate of critical thickness appears to have a film radius dependency similar to that of the experimental measurements. A plot of the ratio of the actual critical film thickness to the predicted upper bound is provided in Figure 8 for numerous foam and emulsion films. The ratios are largely scattered between 0.6 and 0.85, and have a mean value of 0.72 for both foam and emulsion

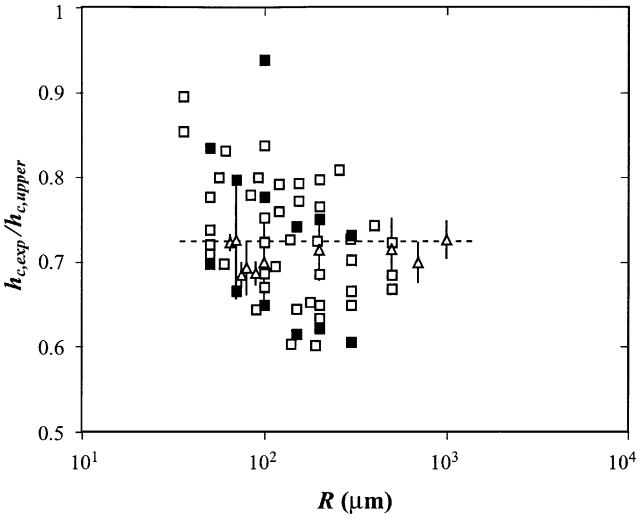

Figure 8. Critical thickness measurements reported on foam (open symbol) and emulsion films (closed symbol) are shown to be approximately 15–40% lower than the upper bound of the critical thickness as calculated from the scaling law. The standard deviation of the foam films reported by Radoev *et al.* (1983) are shown as vertical lines. The dashed line is drawn at the mean value, which is 0.72 for both foam and emulsion films. The data of Traykov (1977), system number 1 is not included in the plot or the calculation of the mean value.

films. If the purpose of this analysis was to demonstrate that a system of approximate equations could be assembled to accurately predict critical thickness values, then a variety of paths can be concocted to achieve such an objective. The possibilities include impeding the zeroth order corrugation growth rate by averaging over all waveforms (Vrij, 1966a; Ivanov *et al.*, 1970), stipulating a different rupture criterion such as a film thickness shift at constant time (Vrij, 1966a) or equating the film thinning and corrugation growth velocities (Radoev *et al.*, 1983), incorporating more accurate film thinning rates (Radoev *et al.*, 1983; Sharma and Ruckenstein, 1987; Coons *et al.*, 2003, 2005b), and adjusting the critical film thickness measurements by replacing the average film thickness with the minimum or maximum film thickness in films with hydrodynamic corrugations (Radoev *et al.*, 1983; Sharma and Ruckenstein, 1987). However, this seems unnecessary and arguably misguided given the approximate nature of the underlying equations.

CONCLUSIONS

A complete solution to the equations bounding the stability and rupture of thin films is provided in the form of a simple scaling law. The scaling law depends on the fundamental physicochemical properties of the film and interface to calculate bounds for the critical thickness and other key film thicknesses, the relevant waveforms associated with instability and rupture, and film lifetimes. As was reported previously (Coons *et al.*, 2005b), critical film thickness measurements on a variety of foam and emulsion films are bounded by the critical thickness scaling equations. It is shown here that the majority of measured critical film thickness values are 15–40% lower than the upper bound critical thickness predicted by the scaling law. Although various paths are available to machinate closer alignments between prediction and experiment, the accuracy provided by the scaling law and the associated constants in Table 1 is acceptable given that the purpose of this analysis is to bound the film drainage and rupture conditions.

NOMENCLATURE

A	non-retarded Hamaker constant, ML^2/t^2
e	percent error as defined by equation (26)
H	local film thickness, L
h	average film thickness, L
$h_{c,lower}$	lower bound critical film thickness, L
$h^*_{c,lower}$	dimensionless lower bound critical film thickness
$h_{c,upper}$	upper bound critical film thickness, L
$h^*_{c,upper}$	dimensionless upper bound critical film thickness
h_t	transition thickness of a wave, L
h^*_t	dimensionless transition thickness of a wave
$h^{max}_{t,0}$	upper bound of the maximum transition thickness, L
$h^*_{t,0}$	dimensionless upper bound of the maximum transition thickness
$h^{max}_{t,1}$	lower bound of the maximum transition thickness, L
$h^*_{t,1}$	dimensionless lower bound of the maximum transition thickness
$h_{t,lower}$	transition thickness of the lower bound critical wave, L
$h^*_{t,lower}$	dimensionless transition thickness of the lower bound critical wave
$h_{t,upper}$	transition thickness of the upper bound critical wave, L
$h^*_{t,upper}$	dimensionless transition thickness of the upper bound critical wave
k_B	Boltzmann's constant, 1.3807×10^{-23} J/°K.
l	dimensionless number of domains provided by MTsR theory
n	dimensionless wave number
P^*	dimensionless drainage pressure
R	film radius, L
R_c	radius of the capillary tube or the radius of curvature at the Plateau border, L
r	radial coordinate, L
S^*	dimensionless parameter in equation (25)
$S^*_{computed}$	dimensionless computed value obtained by solution of the system of equations
$\widehat{S^*}$	dimensionless value calculated from the scaling law
T	absolute temperature, K
$t_{l,lower}$	lower bound of the film lifetime, t
$t_{l,upper}$	upper bound of the film lifetime, t
V_{MTsR}	film thinning velocity given by MTsR theory, equation (13), L/t
V_{Re}	film thinning velocity given by the Reynolds equation, equation (6), L/t
x	dimensionless power defined in equation (25)
y	dimensionless power defined in equation (25)

Greek symbols

α_{crit}	dimensionless root of the critical wave
ΔP	average pressure drop across the film along the radial axis, M/Lt^2
μ	viscosity of the film fluid, M/Lt
σ	interfacial tension, M/t^2
$\tau^*_{l,lower}$	dimensionless lower bound of film lifetime
$\tau^*_{l,upper}$	dimensionless upper bound of film lifetime
ζ	dimensionless corrugation amplitude
ζ_0	initial corrugation amplitude, L

REFERENCES

Coons, J.E., Halley, P.J., McGlashan, S.A. and Tran-Cong, T., 2003, Review of drainage and spontaneous rupture in free standing thin films with tangentially immobile interfaces, *Adv Colloid Interface Sci*, 105(1–3): 3–62.

Coons, J.E., Halley, P.J., McGlashan, S.A. and Tran-Cong, T., 2005a, Bounding the drainage of common thin films, *Colloid Surf A-Physicochem Eng Asp*, doi: 10.1016/j.colsurfa.2005.01.009, in press.

Coons, J.E., Halley, P.J., McGlashan, S.A. and Tran-Cong, T., 2005b, Scaling laws for the critical rupture thickness of common thin films,

Colloid Surf A-Physicochem Eng Asp, doi: 10.1016/j.colsurfa.2005.01.008, in press.
Exerowa, D. and Kolarov, T., 1966, General discussion, *Discuss Faraday Soc*, 42: 60.
Gumerman, R.J. and Homsy, G.M., 1975, The stability of radially bounded thin films, *Chem Eng Commun*, 2(1): 27–36.
Israelachvili, J.N., 1992, *Intermolecular and Surface Forces* (Academic Press, San Diego, USA).
Ivanov, I.B. and Dimitrov, D.S., 1988, Thin film drainage, in *Thin Liquid Films: Fundamentals and Applications* (Marcel Dekker, Inc., New York, USA).
Ivanov, I.B., Radoev, B., Manev, E. and Scheludko, A., 1970, Theory of the critical thickness of rupture of thin liquid films, *Trans Faraday Soc*, 66(569): 1262–1273.
Kumar, K., Nikolov, A.D. and Wasan, D.T., 2002, Effect of film curvature on drainage of thin liquid films, *J Colloid Interface Sci*, 256(1): 194–200.
Manev, E., Scheludko, A. and Exerowa, D., 1974, Effect of surfactant concentration on the critical thickness of liquid films, *Colloid Polym Sci*, 252(7–8): 586–593.
Manev, E., Tsekov, R. and Radoev, B., 1997, Effect of thickness non-homogeneity on the kinetic behaviour of microscopic foam films, *J Dispersion Sci Technol*, 18(6–7): 769–788.
Manev, E.D., Sazdanova, S.V. and Wasan, D.T., 1984, Emulsion and foam stability—the effect of film size on film drainage, *J Colloid Interface Sci*, 97(2): 591–594.
Radoev, B.P., Scheludko, A.D. and Manev, E.D., 1983, Critical thickness of thin liquid films: theory and experiment, *J Colloid Interface Sci*, 95(1): 254–265.
Rao, A.A., Wasan, D.T. and Manev, E.D., 1982, Foam stability—effect of surfactant composition on the drainage of microscopic aqueous films, *Chem Eng Commun*, 15(1–4): 63–81.
Scheludko, A. and Manev, E., 1968, Critical thickness of rupture of chlorobenzene and aniline films, *Trans Faraday Soc*, 64(554P): 1123–1134.
Sharma, A. and Ruckenstein, E., 1987, Stability, critical thickness, and the time of rupture of thinning foam and emulsion films, *Langmuir*, 3(5): 760–768.
Sheludko, A., 1967, Thin liquid films, *Adv Colloid Interface Sci*, 1(4): 391–464.
Traykov, T.T., Manev, E.D. and Ivanov, I.B., 1977, Hydrodynamics of thin liquid films—experimental investigation of effect of surfactants on drainage of emulsion films, *Int J Multiphase Flow*, 3(5): 485–494.
Vrij, A., 1966a, Possible mechanism for the spontaneous rupture of thin, free liquid films, *Discuss Faraday Soc*, 42: 23–33.
Vrij, A., 1966b, General discussion, *Discuss Faraday Soc*, 42: 60.

ACKNOWLEDGEMENTS

This work was supported in part by the U.S. Department of Energy under contract W-7405-ENG-36.

This paper was presented at the 7th World Congress of Chemical Engineering held in Glasgow, UK, 10–14 July 2005. The manuscript was received 15 December 2004 and accepted for publication 18 March 2005.